31st Annual International Conference of the IEEE EMBS
Minneapolis, Minnesota, USA, September 2-6, 2009

# FOUR-DIMENSIONAL QUANTITATIVE ANALYSIS OF THE GAIT OF MUTANT MICE USING COARSE-GRAINED MOTION CAPTURE

S. Oota, *Member IEEE*, K. Mekada, Y. Fujita, J. Humphries, K. Fukami-Kobayashi, Y. Obata, T. Rowe and A. Yoshiki

***Abstract*— To analyze an abnormal gait pattern in mutant mice (*Hugger*), we conducted coarse-grained motion capture. Using a simple retroreflective marker-based approach, we could detect high-resolution mutant-specific gait patterns. The phenotypic gait patterns are caused by extreme vertical motion of limbs, revealing inefficient motor functions. To elucidate the inefficiency, we developed a musculoskeletal computer model of the mouse hindlimb based on X-ray CT data. By integrating motion data with the model, we determined mutant-specific musculotendon lengths, suggesting that three major muscles were involved in the abnormal gait. This approach worked well on laboratory mice, which were putatively too small to be motion capture subjects. Motion capture technology was originally developed for human study, and our approach may help fill neuroscience gaps between mouse and human behavioral phenotypes.**

## I. Introduction

Behaviors of laboratory mice are important phenotypes, especially in neuroscience [1, 2]. Traditionally, such phenotypes have been described through domain-specific contextual paradigms: sensory abilities, learning and memory, feeding and drinking, reproductive behavior, social behavior, and emotional behaviors [1]. Although many sophisticated behavior tests have been developed [1], existing methodologies are spatiotemporally primitive. Thus, we cannot exclude the possibility that subtle, but important, behavioral phenotypes have not been detected. From a physical perspective, behaviors can be reduced to a set of motion patterns, which are theoretically measurable in a paradigm-independent manner [3].

In the 1980's, a practical technology to directly measure motions emerged: motion capture technology [4, 5]. Using motion capture systems, somatic motor functions of human and relatively large animals have been elaborated. The applications have been wide ranging: psychology [6], socio-behavioral science [7], genetic disorders [8], psychiatry [9], biomechanics [10-12], and neuroscience [13-17]. The precise, comprehensive, and objective motion capture data have made significant impacts on the above fields. In terms of ethics and cost, however, human and relatively large animals (even rats) are deemed inappropriate for extensive genetic studies. Thus, if motion capture technology can be applied to laboratory mice, putatively too small to be motion capture subjects, an immense impact on the life sciences may follow. As examples: (1) over 400 inbred mouse strains are available for biomedical research [18]; (2) knockout mouse projects are underway to create targeted mutations in every gene for the study of human gene functions and diseases [19]; and (3) accumulated human motion data [6-10, 13-17] may shed light on behavioral phenotype correlations between mice and humans.

We conducted comprehensive, coarse-grained motion capture on laboratory mutant mice, dubbed Mouse Motion Capture (MMoCap). In this paper, we analyzed an abnormal gait pattern of Hugger Rbrc, $hug^{Rbrc}$, [20-22], which is a recessive spontaneous mutant mouse recovered at RIKEN BioResource Center (Tsukuba, Japan) with a C57BL/6JJcl background. Briefly, homozygous $hug^{Rbrc}$ / $hug^{Rbrc}$ mutants show an abnormal gait: a duck-like walking pattern (lifting a hindlimb higher than normal and sometimes shaking it before setting the hindlimb down), while heterozygous $hug^{Rbrc}$ /+ mice are perceived as normal. The homozygous mutant mice also have smaller eyes than those of heterozygous mice due to degeneration of the retina [21, 22]. These behavioral and retinal phenotypes, in addition to the genetic linkage map on Chromosome 19, completely overlap with those of hugger mutant mice reported in previous studies. However, quantitative analyses on the phenotypic gait pattern had never been performed. Our primary purpose is to obtain detailed quantitative traits of the abnormality.

We employed an optical motion capture system with 6–8 cameras to capture mouse motions. Eight retroreflective markers were used to detect motions (Fig. 1a). A major difference between MMoCap and conventional motion capture systems is the number of markers. MMoCap marker density is coarse grained, as the smallest retroreflective markers (diameter 2.4 mm) were still large and heavy for laboratory mice, and at most nine markers could be used on each mouse (Fig. 1a). In contrast, conventional motion capture systems typically require 10–40 markers for a whole body. Furthermore, mouse marker positions were severely restricted so that the mouse body did not obstruct the markers from the cameras. For example, markers on the feet did not provide consistent data. As shown below, however,

Manuscript received April 7, 2009. This work was supported by the National Science Foundation (IIS-0208675) and KAKENHI from the Japan Society for the Promotion of Science: Grant-in-Aid for Exploratory Research (17650122) and Grant-in-Aid for Scientific Research (C) (19570051).

S. Oota, K. Mekada, K. F-Kobayashi, Y. Obata, and A. Yoshiki are with RIKEN BioResource Center, Tsukuba, Japan (phone: +81-29-836-9039; fax: +81-29-836-9077; e-mail: oota@riken.jp).

Y. Fujita is with NAC Image Technology, Tokyo 102-0075, JAPAN.

J. Humphries and T. Rowe are with The University of Texas at Austin, Austin, TX 78712-0254, USA.

this small number of markers did provide informative and consistent data. Our experimental protocols, including animals, were approved by the Animal Experiment Committee of the RIKEN Tsukuba Institute.

## II. Arena: Space for Mouse Gating

A rectangular stainless steel plate (150 cm × 100 cm painted matte black) comprised the mouse-gaiting arena. The motion capture coordinate system focused on the arena with the x- and y-axes set along the long and short sides of the plate, respectively. The z-axis was set perpendicular to the rectangle. In the arena, a removable beam was installed (Fig. 2a), which sloped approximately 18 degrees above level, and aligned with the x-axis of the motion capture system. The slope was empirically determined in terms of mouse mobility on the beam. Using the sloped beam and the arena's rectangle surface, three types of gaiting motion (level, uphill, and downhill) data could be collected.

The primary interest was in height variation between adjacent motion peaks. To obtain relative z-coordinates (heights) of mice on the sloped beam (Fig. 2a), we standardized the z-coordinates to the corresponding x- and y-coordinates by

$$z' = z - \tan\left|\arcsin\left(\frac{t-s}{l}\right)\right| x, \tag{1}$$

where $t$, $s$, and $l$ are the height of the short leg of the beam, the long leg, and the length between the two legs, respectively (in our case, $l$ = 820 mm; $s$ = 87 mm; $t$ = 235 mm).

Marker stride distance was calculated by the following equation:

$$\hat{l}_{\text{stride}} = \sqrt{(x_2 - x_1)^2 + (y_2 - y_1)^2}, \tag{2}$$

where $(x_1, y_1)$ and $(x_2, y_2)$ are x–y coordinates corresponding to upward or downward peaks. We define a stride as either an "upward stride" if $(x_1, y_1)$ and $(x_2, y_2)$ are downward and upward peaks, respectively, or as a "downward stride" if $(x_1, y_1)$ and $(x_2, y_2)$ are upward and downward peaks, respectively. A corresponding marker stride speed was calculated by dividing a marker stride by the duration between peaks. Uphill and downhill strides on the sloped beam (Fig. 2a) were distinguished by time sequence data along the x- and z-coordinates, as well as through filmed images.

## III. Results

### A. Marker-based analyses

Mouse motions were standardized according to their proportions along a mean length of three-dimensional cubic spline curves interpolating the three base markers (Fig. 1a): *e.g.*, 0.1 indicates marker translocation of up to one tenth of the interpolated curve length. Fig. 1b shows a comparison of standardized mean marker strides of fore and hind limbs between and within mutant (*hug/hug*) and normal (*hug/+*) mice. Neither comparison showed a significant difference. Note that mean strides of the fore and hind limbs should be nearly identical if slippage between limb and ground is ignored. Although fore and hind limb markers were placed on the elbow and ankle (*i.e.*, not on feet), the results show that marker strides closely approximated actual limb strides. Fig. 1c shows standardized mean height variations of the head (Head), back (Back1 and Back2), forelimb (Forelimb), and hindlimb (Hindlimb and Tail1) markers during gaits. The height variations are indicated as the mean of vertical differences between neighboring (upward and downward) peaks. All markers showed highly significant differences in standardized mean height variations between mutant and normal mice, in contrast with the limb stride pattern results (Fig. 1b). Fig. 1d shows a comparison of standardized mean marker speeds between mutant and normal mice. Note that Head, Back1, Back2, and Tail1 did not show significant differences in speed within mutant and normal mice (detail in tables S1, S2, and S3 - see Appendix). Since the four markers placed on the same bodies were propelled by forelimbs and hindlimbs, their standardized mean speeds were expected to be nearly identical. These results show that standardized data are informative and fairly consistent in spite of potential errors, *e.g.*, inaccurate marker positions or mislabeled motion data.

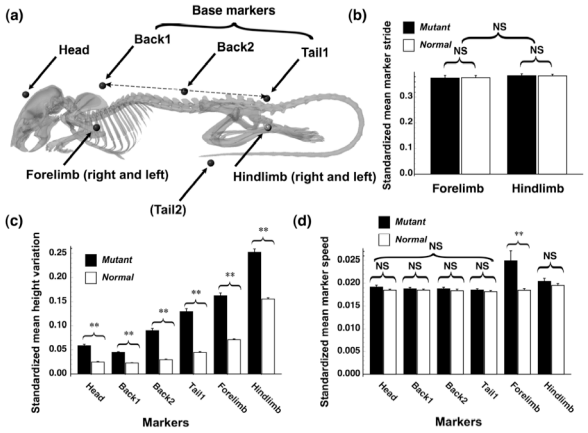


Figure 1 (a) Retroreflective marker positions; only the left side is shown. Back1, Back2, and Tail1 markers are base markers. Data from Tail2 were not used. (b) Comparison of standardized mean marker strides of fore and hind limbs between and within mutant and normal mice. Neither comparison shows significant differences. (c) Standardized mean height variation of markers between mutant and normal mice. All markers showed significant differences between mutant and normal mice. (d) Comparison of standardized mean marker speeds between and within mutant and normal mice. Head, Back1, Back2, Tail1, and Hindlimb markers did not show significant difference in speed between and within mutant and normal mice; however, Forelimb maker showed a significant difference in speed. See tables S1, S2, and S3 for details. NS and ** indicate insignificant or significant differences, respectively, at the 5% level determined by a two-tailed t test. Error bars indicate standard errors of the means (s.e.m.).

As shown in Fig. 1c, to produce the same propulsion, mutant mice lifted their limbs approximately twice as high as normal mice, thus suggesting an inefficient gait pattern in mutant mice. We defined the efficiency of stride as a

logarithm of the ratio of horizontal to vertical limb motion. Except for hindlimb efficiency in the level state, all the data clearly show lower efficiency in mutant than in normal mice (Fig. 2b).

### B. Model-based analyses

While this marker position-based analysis is powerful, we missed certain aspects of the fourth dimension of the data. The motion data apparently have a clear structure that is associated with biomechanical constraints, *i.e.*, degree of freedom, motion range, morphology, and neuronal interactions. However, the marker position-based approach treated the data as a set of independent trajectories. To overcome this problem, we constructed a computational model (a musculoskeletal model). Using inverse kinematics [23], we were able to map the motion data in the musculoskeletal model and estimate subject motions in terms of both skeletal and muscle structure. We deemed it easier to analyze the musculoskeletal model, which is a purely mathematical entity, than to attempt to analyze the actual mouse.

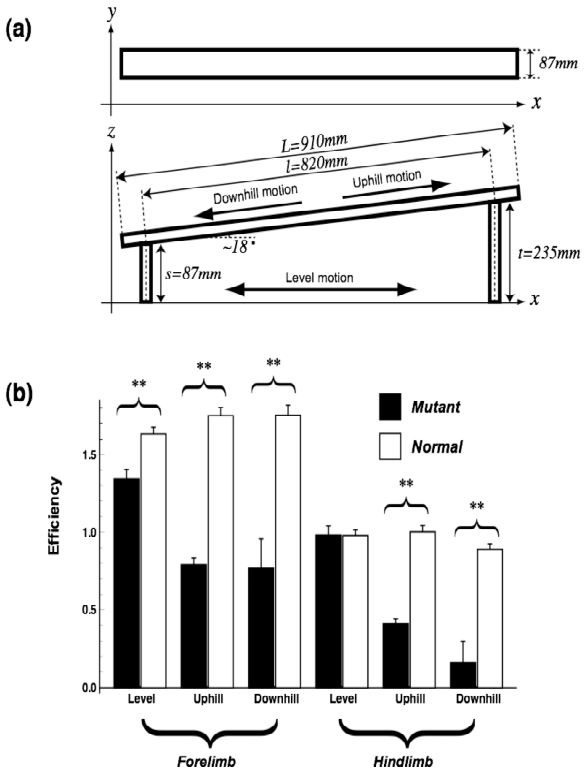


Figure 2 (a) Sloped beam used in the motion capture. The beam was aligned with the x coordinate of the motion capture system. Arrows indicate schematic motions of mice on the level surface (Level motion) and on the beam (Downhill and Uphill motions). (b) Efficiency of marker strides. Uphill and Downhill data show lower efficiency in mutant than normal, as well as Forelimb level data. ** indicate significant differences at the 5% level determined by two-tailed t test. Error bars indicate s.e.m.

We performed detailed motion capture on the mouse hindlimb using 6 retroreflective markers. We obtained 349,710 frames of hindlimb motion capture data and mapped the data to the hindlimb musculoskeletal computer model (Fig. 3a). Six musculotendon lengths in the right hindlimb were assessed using the SIMM software (MusculoGraphics, Inc, Chicago, IL USA; Fig. 3b) [24]. In the three mutant muscles (tensor fasciae latae muscle, superficial gluteal muscle, and biceps femoris muscle/short head), characteristic patterns were observed in comparison with normal muscles. Meanwhile, three other muscles (semitendinous, biceps femoris muscle/long head, and rectus femoris muscle) did not show such anomalous signals. These results suggest that at least three muscles are involved in the mutant-specific gait pattern.

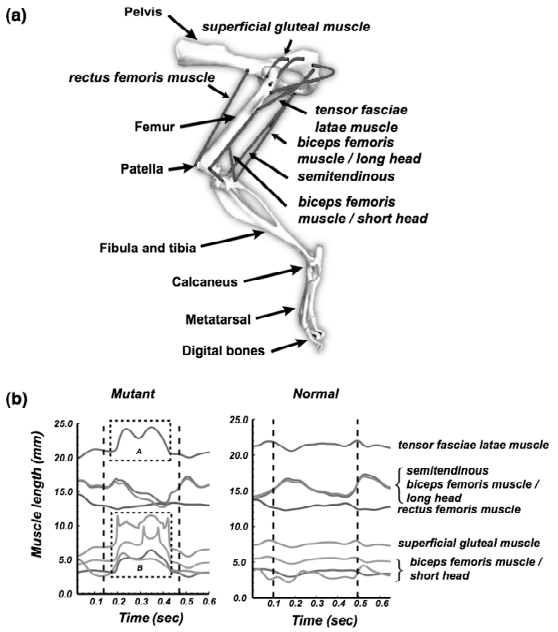


Figure 3 (a) Partial musculoskeletal model of mouse hind limb. The skeleton model was constructed by segmenting X-ray scanning volume data based on the anatomical structure. Grey lines represent six major muscles of the upper hind limb, which are indicated by italic letters. They were modeled as a musculotendon actuator model. Note that superficial gluteal muscle is represented by three actuator models. The nomenclature of Iwaki, Yamashita, and Hayakawa (2001) was followed. (b) Comparison of changes of major hindlimb musculotendon lengths between mutant and normal mice. In three mutant muscles (tensor fasciae latae muscle, superficial gluteal muscle, and biceps femoris muscle/short head), characteristic patterns were observed in comparison with normal muscles (indicated by rectangles A and B). The other three muscles (semitendinous, biceps femoris muscle/long head, and rectus femoris muscle) did not show signal differences. Vertical broken lines indicate upward peaks of markers on the ankles, i.e., the region flanked by the two broken lines corresponds to a single stride.

## IV. DISCUSSION

Our approach provided an anatomical insight into the abnormal gait, which may be considerably useful in subsequent genetic and physiological studies. While the easily recognizable hindlimb motion of Hugger mice was qualitatively described by others [20-22], indistinct mutant-specific phenotypic motions (*e.g.*, the head, back, hip, and forelimbs) have not been reported previously. This suggests that conventional methods do not have sufficient power to detect subtle motion signals.

Laboratory mice are excellent human disease model organisms due to the availability of comprehensive genetic tools. There are many human neurological diseases that are associated with mouse behavioral phenotypes, e.g., Huntington's disease [25], Parkinson's disease [26], and schizophrenia [27]. So far, conceptual analogies have been

used to relieve the difficulties of extrapolation between humans and mice. However, it has been difficult to authenticate the extrapolation because the true biomechanical reasons for a phenotypic behavior have been unknown. Since motion capture technology was originally developed for analyzing human complex behavior, an abundance of information correlating human phenotypes has been accumulated [6-10, 13-17]. Therefore, additional quantitative analyses of motion capture data of laboratory mice will potentially fill gaps between mice and humans, which are especially important to neuroscience studies.

Conventional behavioral tests may answer "how," but do not answer "why" in a direct manner. If we can obtain biomechanical information on "why," association of behavioral phenotype with genotype will be easier. The proposed coarse-grained motion capture approach, MMoCap, can provide an insight into musculotendon anatomical structures and answers to "why" questions.

## V. Conclusion

Coarse-grained motion capture was successfully applied to mutant laboratory mice, which are significantly useful for studies of human neurological disorders. We also developed the first mutant mouse musculoskeletal model of the hind limb, and obtained insightful data on abnormal gait patterns through the inverse kinematics.

## Appendix

Tables S1-S3 are provided as supporting online material at http://homepage.mac.com/satoshi.oota/EMBC2009/FileSharing41.html (Password: MMoCap).

## Acknowledgment

We thank Jessie Maisano and Sanae Yokota for undertaking the burdensome segmentation tasks; Fujimi Arai and Ayumi Murakami for technical assistance with mice; and Kazuo Moriwaki, Takashi Gojobori, Naruya Saitou, Kazuhiro Kawamura, and Tadashi Tsuda for useful discussions.

## References

[1] J.N. Crawley, *What's wrong with my mouse*, New York, USA: John Wiley & Sons, 2000.

[2] T. Nakashiba, J.Z. Young, T.J. McHugh, D. Buhl, and S. Tonegawa, "Transgenic Inhibition of Synaptic Transmission Reveals Role of CA3 Output in Hippocampal Learning," *Science*, vol. 319, (no. 5867), pp. 1260-1264, 2008.

[3] A.A. Biewener, *Animal Locomotion*: Oxford University Press, 2003.

[4] T.W. Calvert, J. Chapman, and A. Patla, "Aspects of the kinematic simulation of human movement," *IEEE Computer Graphics and Applications*, vol. 2, pp. 41-50 1982.

[5] C.M. Ginsberg and D. Maxwell, "Graphical marionette," *ACM SIGGRAPH/SIGART Workshop on Motion*, pp. 172-179, 1983.

[6] A.L. Yuille and N.M. Grzywacz, "A computational theory for the perception of coherent visual motion," *Nature*, vol. 333, pp. 71-4, 1988.

[7] W.M. Brown, L. Cronk, K. Grochow, A. Jacobson, C.K. Liu, Z. Lalosević, and R. Trivers, "Dance reveals symmetry especially in young men," *Nature*, vol. 438, pp. 1148-50, 2005.

[8] M. Kubo and B. Ulrich, "Coordination of pelvis-HAT (head, arms and trunk) in anterior–posterior and medio-lateral directions during treadmill gait in preadolescents with/without Down syndrome," *Gait & Posture*, vol. 23, (no. 4), pp. 512-518, 2005.

[9] A. Norman, "Is There a Future for Depression Digital Motion Constructs in Psychiatry?," *CyberPsychology & Behavior*, vol. 4, (no. 4), pp. 457-463, 2001.

[10] R.D. Trumbower and P.D. Faghri, "Kinematic analyses of semireclined leg cycling in able-bodied and spinal cord injured individuals," *Spinal Cord*, vol. 43, pp. 543-9, 2005.

[11] Y. Nakamura, K. Yamane, and A. Murai, "Macroscopic Modeling and Identification of the Human Neuromuscular Network," *in Proc. of the IEEE EMBS '06 28th Annual International Conference*, pp. 99-105, 2006.

[12] J.H. Ryu, N. Miyata, M. Kouchi, M. Mochimaru, and K.H. Lee, "Analysis of skin movement with respect to flexional bone motion using MR images of a hand," *J Biomech*, vol. 39, (no. 5), pp. 844-52, 2006.

[13] K.L. Siegel and L.V. Metman, "Effects of Bilateral Posteroventral Pallidotomy on Gait of Subjects With Parkinson Disease," *Arch Neurol*, vol. 57, (no. 2), pp. 198-204, February 1 2000.

[14] J. Zakotnik, T. Matheson, and V. Dürr, "A posture optimization algorithm for model-based motion capture of movement sequences," *Journal of Neuroscience Methods*, vol. 135, (no. 1-2), pp. 43-54, 2003.

[15] D. Jokisch, I. Daum, and N.F. Troje, "Self recognition versus recognition of others by biological motion: viewpoint-dependent effects," *Perception*, vol. 35, (no. 7), pp. 911-920, 2006.

[16] L. Hamilton, R. Franklin, and N. Jeffery, "Development of a universal measure of quadrupedal forelimb-hindlimb coordination using digital motion capture and computerised analysis," *BMC Neuroscience*, vol. 8, (no. 1), pp. 77, 2007.

[17] P. Neri, J.Y. Luu, and D.M. Levi, "Meaningful interactions can enhance visual discrimination of human agents," *Nat Neurosci*, vol. 9, pp. 1186-92, 2006.

[18] J.A. Beck, S. Lloyd, M. Hafezparast, M. Lennon-Pierce, J.T. Eppig, M.F. Festing, and E.M. Fisher, "Genealogies of mouse inbred strains," *Nat Genet*, vol. 24, (no. 1), pp. 23-5, Jan 2000.

[19] F.S. Collins, J. Rossant, and W. Wurst, "A mouse for all reasons," *Cell*, vol. 128, (no. 1), pp. 9-13, Jan 12 2007.

[20] V.D. Bode, "Hugger, a new neurological mutant of the mouse," *Genetics*, vol. 94, pp. S10, 1980.

[21] R.L. Sidman, M. Tang, B. Kosaras, S.J. Phillips, and B.A. Taylor, "Mapping and retinal phenotype of the hugger mutation in the mouse," *Mamm Genome*, vol. 8, pp. 399-402, 1997.

[22] P. Neumann, C. Kerr, and R.L. Sidman, "Hugger: a new neurological mutant with retinal malformation," *Mouse News Lett.*, vol. 81, pp. 60 1988.

[23] D.R. Baker and C.W. Wampler, II, "On the Inverse Kinematics of Redundant Manipulators," *The International Journal of Robotics Research*, vol. 7, (no. 2), pp. 3-21, April 1 1988.

[24] S.L. Delp and J.P. Loan, "A graphics-based software system to develop and analyze models of musculoskeletal structures," *Comput Biol Med*, vol. 25, pp. 21-34, 1995.

[25] M.Y. Heng, S.J. Tallaksen-Greene, P.J. Detloff, and R.L. Albin, "Longitudinal evaluation of the Hdh(CAG)150 knock-in murine model of Huntington's disease," *J Neurosci*, vol. 27, (no. 34), pp. 8989-98, Aug 22 2007.

[26] K.M. Strauss, L.M. Martins, H. Plun-Favreau, F.P. Marx, S. Kautzmann, D. Berg, T. Gasser, Z. Wszolek, T. Muller, A. Bornemann, H. Wolburg, J. Downward, O. Riess, J.B. Schulz, and R. Kruger, "Loss of function mutations in the gene encoding Omi/HtrA2 in Parkinson's disease," *Hum Mol Genet*, vol. 14, (no. 15), pp. 2099-111, Aug 1 2005.

[27] M. Kvajo, H. McKellar, P.A. Arguello, L.J. Drew, H. Moore, A.B. MacDermott, M. Karayiorgou, and J.A. Gogos, "A mutation in mouse Disc1 that models a schizophrenia risk allele leads to specific alterations in neuronal architecture and cognition," *Proc Natl Acad Sci U S A*, vol. 105, (no. 19), pp. 7076-81, May 13 2008.